Thermodynamic Calculations on the Chemical Vapor Deposition of Silicon Nitride and Silicon from Silane and Chlorinated Silanes

Frank Einar Kruis, Brian Scarlett, Robert A. Bauer, and Joop Schoonman*

Laboratory of Particle Technology and Laboratory of Inorganic Chemistry, Faculty of Chemical
Engineering and Materials Science, Delft University of Technology, 2628 BL Delft, The Netherlands

After a discussion of the thermochemical values of the Si–H–Cl–N system which occur in the literature, CVD phase diagrams are presented which include contours of constant deposition efficiency. The temperature range considered is from 800 to 2600 K. A number of chlorinated silanes as well as silane can be used as a silicon source, while ammonia is used as the nitrogen source. The effects of pressure variation and dilution by nitrogen and hydrogen are also included. Some initial calculations concerning silicon diimide are made. The CVD phase diagrams are used to describe several mechanisms occurring during the formation of silicon nitride from the gas phase. [Key words: thermodynamics, silicon nitride, chemical vapor deposition, phase diagrams, silanes.]

I. Introduction

SILICON NITRIDE is receiving increasing attention as a material for structural applications, especially as coatings and precursor ceramic powders. This is due to its superior properties at high temperatures, extreme hardness, oxidation resistance, and mechanical strength. The term "chemical vapor deposition" is often encountered in this field, and comprises the reaction of one or more gaseous precursors to form a condensed phase or phases, and gaseous products. "Chemical vapor precipitation" is a CVD process which produces a powder.

Si_3N_4 is not easily sintered, for several reasons: the strong covalent bond of Si–N, the low self-diffusivity of pure Si_3N_4, and decomposition above 2100 K. Practical problems often encountered in the synthesis include oxygen contamination, resulting in a SiO_2 layer which can constitute a large portion of the powder when it is very fine, chlorine contamination when chlorinated silanes are used as a source, hydrogen inclusions, metallic impurities resulting from the corrosive properties of the product gas, codeposition with silicon, and agglomeration of fine particles.

Thermodynamic calculations are a useful tool in understanding a specific CVD system and in optimizing the process conditions. A thermodynamic analysis must be completed before the kinetic effects are considered.[1] Furthermore, kinetic models often include a thermodynamic term. In the case of homogeneous nucleation of ceramic powders, the supersaturation which is the driving force for the process must be known.

The main limitations to the validity of these thermodynamic calculations result from the inaccuracy or lack of the thermodynamic data and, of course, from the assumption

that equilibrium is achieved. Concerning the thermodynamic data, a 5% change in the heat of formation of a major species can change the deposition efficiency by a factor of 2.[2]

The result of this work will be presented in the form of CVD phase diagrams, which depict which solid phases would deposit as a function of the experimental variables such as temperature and the input gases. These diagrams give phase boundaries and also the deposition efficiency of the Si_3N_4 and Si phases, and are considered the simplest and clearest way to present the thermodynamic results.

The purpose of this work is to calculate a number of CVD phase diagrams in the Si–H–Cl–N system. After a discussion of the thermochemical data, some new data are adopted in the calculations. Some assumptions were made concerning the silicon diimide, which has never been included in thermodynamic calculations before. High temperatures (2600 K) are included, together with different pressures and dilution by hydrogen or nitrogen. The phase diagrams are also used to describe some mechanisms in the formation of Si_3N_4 from the gas phase, and make some recommendations concerning favorable synthesis paths.

II. Review of Previous Work

The Si–H–Cl system has been extensively studied because of its use in the electronics industry. The literature can be divided into work on thermochemical data and on chemical equilibrium. In both cases there are experimental, theoretical, and review articles. The Si–H–Cl–N system has been studied less, being of less practical use to industry and being more difficult. The reason for this will be clarified later in this article.

The thermochemical data on the Si–H–Cl system will be dealt with in the next section. It suffices here to give some general overview of the work, which consists of some older calorimetric measurements and more recent mass spectrometry studies. Reviews of these works are given by JANAF,[3] Walsh,[4] and Ho.[5] Recent theoretical work by Ho[5,6] concerns ab initio calculations and reaction cross sections from MS measurements by Boo[7] and Weber.[8]

Equilibrium calculations on the Si–H–Cl system were made by Hunt[9–11] and Herrick.[12] Hunt[11] calculates up to 1700 K with few species, Herrick[12] up to 3000 K with most known species.

Experimental equilibrium experiments on the Si–H–Cl system are made by Ban[13] and Woodruff.[14] Only a few temperatures were investigated. There are fewer articles on the Si–H–Cl–N system. There are some equilibrium calculations on specific reactors, for example the hybrid plasma reactor by Yoshida,[15] the N_2 plasma reactor by Li,[16] and the liquid NH_3 route by Crosbie.[17] Experimental papers are scarce, for example the mass spectrometric study of intermediates in the $SiCl_4–NH_3$ system by Lin.[18] General papers on the Si–H–Cl–N system, especially deposition efficiencies, are by Paretta[19] and Kingon.[1] The last article is an important article, in which the results are made clearly visible by CVD phase diagrams for several source gases, various pressures, and carrier gases. The temperature range is up to 1800 K.

III. Discussion of Thermochemical Data

It has been shown in the literature,[2] and becomes clear in our own calculations, that the equilibrium calculations are very sensitive to variations in the standard heat of formation of a particular species. It has been pointed out by several workers, especially Walsh[4] and Ho,[5] that some literature study is needed before attempting calculations, as standard tables like JANAF[3] and CATCH[20] might not contain the latest results. Thus, some CATCH tabulations originate from the beginning of this century, which causes the work of Bell[21] to be unreliable.

In Table I a summary is given of the literature values of the standard heat of formation of the species considered in this work. Calculated, experimental, and review values are given, as well as the values used in this work.

As for SiH_4, SiH_3Cl, SiH_2Cl_2, $SiHCl_3$, and $SiCl_4$, the values given in the review of Walsh[4] were used. He considers the Farber[22] values to be the most reliable. From the silicon subchlorides, only the value of $SiCl_2$ is well established. Walsh[4] and Ho[5] show that the measurements of Farber[23] are unreliable, as well as the JANAF tabulations,[3] which are based on it. As for SiCl, both the Walsh[4] and the Weber[8] review take the median of some experimental values. Taking these values and the two calculated values by Ho[5] and Weber,[8] the median is close to the value calculated by Ho[5] and the value recommended by Walsh.[4] There is considerable disagreement over the value for $SiCl_3$. The Farber[23] value, adopted by JANAF,[3] is rejected by Walsh[4] and Ho.[5] We have taken the median of the values of Steele,[24] Wang,[25] Cadman,[26] Walsh,[27] and Ho.[5]

Only recently, a number of experimental and theoretical studies have appeared on the SiH species ($n = 1, 2, 3$), which are important intermediates in pyrolysis reactions. Boo[7] has experimentally confirmed the JANAF[3] value of ΔH_{298} (SiH), and rejects the value measured by Carlson.[28] The JANAF value for SiH was used in this work. The value for SiH_2 is reviewed and measured by Boo.[7] He discards the values by Walsh[27] and Pople.[27] His result is in good agreement with Ho,[5] Shin,[30] and Berkowitz,[31] so this value was accepted. The value of the standard heat of formation for SiH_3 of Boo[7] is also accepted, which is in good agreement with the calculations by Ho[5] and Pople.[29]

The chlorinated intermediates SiHCl, $SiHCl_2$, and SiH_2Cl are not experimentally characterized. The only reliable values are calculations by Ho.[5]

The condensed phases present more problems. The only form present in the JANAF tables is the α form of Si_3N_4, which was thus used. In reality there are three known forms: amorphous Si_3N_4 which deposits below 1500 K, α-Si_3N_4 between 1500 and 1650 K, and at still higher temperature β-Si_3N_4. From a thermodynamic viewpoint it can be argued that, when the thermodynamic properties are different, the transition temperatures depend on the chemical species and concentrations, and also on the pressure.

Polymeric intermediates like $Si(NH)_2$ and $Si(NH_2)Cl$ are known to exist at lower temperatures and might be relatively stable, Mazdiyasni and Cooke[32] suggest up to 1470 K, but unfortunately there are no experimental thermodynamic data on these species. This limits the reliability of the phase diagrams at lower temperatures. We attempted the inclusion of

Table I. Overview of Standard Enthalpy of Formation, ΔH_{298}, of Si–H–Cl–N Species

Species	This work	Literature*
		ΔH_{298} (kJ/mol)
$SiCl_4$	−662.75	−662.75,[3,39] −655.63,[9,40] −609.61(c),[21] −662.75(r)[4]
$SiHCl_3$	−499.2	−496.22(c),[3] −489.11(c),[9] −499.2,[22] −494.1,[41] −499.15(r),[4] −489.53(c),[5] −497.3(r)[5]
SiH_2Cl_2	−315.49	−320.49(c),[3] −313.8,[9,42] −315.05,[22] −315.05(r),[4] −311.71(c)[5]
SiH_3Cl	−135.6	−141.84(c),[3] −142.26,[9] −135.6,[22] −135.6(r),[4] −134.72(c)[5]
SiH_4	34.31	34.31,[3,43] 30.54[9]
$SiCl_3$	−326.4	−390.37,[3,23] −288.70,[24] >−326.35,[9] −338.90,[25] −366.1,[26] −317.98,[27] −334.72(r),[4] −320.08(c),[5] >−357.0,[11] −326.35(r)[8]
$SiCl_2$	−168.62	−168.62(r),[3] −167.36,[44] −168.20,[45] −168.20,[46] −159.83,[9] 170.71,[23] −165.27,[27] −168.60,[4] −157.32(c),[5] −168.6(r)[8]
$SiCl$	158.9	198.32,[3,23] 191.21,[9] 195.81,[27] 154.81(r),[4] 158.57(c),[5] 189.53(c),[47] 183.9(c, r)[8]
Si	450.0	3
Si_2	589.9	3
Si_3	636.0	3
Cl	121.302	3
H	217.999	3
H_2	0.0	3
Cl_2	0.0	3
HCl	−92.312	3
SiH	376.66	376.66,[3] 341.83,[28] 376.56,[27] 383.67(c),[5] 369.45(c),[29] 376.56[7]
SiH_2	288.7	242.67,[27] 284.93(c),[5] 265.27(c),[29] 288.70,[30] 285.35,[31] 288.70[7]
SiH_3	202.92	194.14,[27] 200.00(c),[5] 197.90(c),[29] 202.92[7]
SiHCl	71.13	40.17,[21] 71.13[5]
$SiHCl_2$	−143.51	−165.27,[21] −143.51[5]
SiH_2Cl	32.64	8.37,[21] 32.64[5]
N	472.68	3
N_2	0.0	3
N_3	414.22	3
NH	376.56	3
N_2H_2	212.97	3
NH_3	−45.898	3
SiN	372.38	3
Si_2N	397.48	3
Si(l)	48.470	3
Si(s)	0.0	3
$Si_3N_4(s)$	−744.752	3
$NH_4Cl(s)$	−314.553	3
$N_2H_4(l)$	50.626	3
$Si(NH)_2$	−355.6	17

*c = calculated; r = review.

Si(NH)$_2$ by using an estimation by V. Parker of the U.S. National Bureau of Standards, in the work of Crosbie,[17] of the standard enthalpy and the standard entropy of Si(NH)$_2$. Unfortunately the error range of these values is large. We will discuss these values further. The heat capacity is unknown; an estimated value of the heat capacity at 298 K of 41.5 kJ/mol was used, based on the fact that heat capacity expressed in kJ/g is the same for both Si and Si$_3$N$_4$. Further, the temperature dependence of the heat capacity of Si(NH)$_2$ was assumed to be the same as that of Si$_3$N$_4$.

Still some data are needed, namely the standard entropy and the heat capacity of SiH, SiH$_2$, SiH$_3$, SiHCl, SiH$_2$Cl, and SiHCl$_2$. They have been interpolated, using the method described in Hunt.[33] There is a nearly linear relationship between the logarithms of the entropy and molecular weight for similar series of compounds. The heat capacities are linearly interpolated. The results are given in Table II.

All of the other heat capacities were interpolated from the JANAF tables, mostly using two temperature ranges because of the large total range. The error is within 0.5%.

To test the validity of the thermochemical data, the experimental data of Woodruff[14] on the deposition efficiency in the Si–H–Cl system were used. As the new thermodynamic data comprise no nitrogen atoms, this was thought to be sufficient. Also, there are no reliable experimental data on deposition efficiencies in the Si–Cl–H–N system. Two datasets were tested: one including all species in Table I, and one excluding the five radicals with uncertain thermochemical data—SiH$_2$, SiH$_3$, SiHCl, SiH$_2$Cl, and SiHCl$_2$. An example result is shown in Fig. 1. At this relatively low temperature the difference between the two datasets is within 0.2%. The calculated deposition efficiency is slightly below the experimental values, but agrees quite well. It is to be expected that at high temperatures the radicals will become important, so the complete dataset was used for calculating the phase diagrams.

IV. Method of Calculation

The computer program SOLGASMIX by G. Eriksson[34] was converted from supercomputer FORTRAN code to MS FORTRAN code. The program input requires atomic composition of the species, input concentrations, and thermochemical values like those of the standard heat of formation, the standard entropy, and the specific heat as a function of temperature. The calculated equilibrium composition includes condensed and gaseous species.

In most cases, the results are presented as CVD phase diagrams as a function of temperature and the Si/(Si + N) ratio of the input gas, except in the case of N$_2$ dilution, where the Si/(Si + NH$_3$) ratio is used. This ratio is 0.5 for a 1 mol SiH$_2$Cl$_2$ and 1 mol NH$_3$ mixture, and decreases when the NH$_3$ concentration in the input gas increases. The silicon source gas, the system pressure, and the concentration of the carrier gas were varied systematically. Because of interest in LPCVD and HPCVD, a wide range of pressures was studied. The carrier gas is present in constant abundance to the rest of the input gases, e.g., the total number of moles of H$_2$ divided by the sum of the total number of moles of SiH$_2$Cl$_2$ and NH$_3$. This method, adopted from Kingon,[1] was found to be the most clear.

V. Results

(1) The Si–H–Cl–N System at 1 bar

In Fig. 2 the CVD phase diagrams of SiH$_4$, SiH$_2$Cl$_2$, SiHCl$_3$, and SiCl$_4$ at 1 bar are shown, including the deposition efficiency. In the SiH$_4$/NH$_3$ system there is a large region where codeposition of Si with Si$_3$N$_4$ occurs, when insufficient NH$_3$ is added to the system. When the chlorine content of the silane compound increases, so going toward SiCl$_4$, the formation of stable gas-phase species which contain silicon and chlorine, like SiCl$_2$, becomes possible. In the case of SiH$_4$/NH$_3$, there are no stable gaseous silicon-bearing species; even the source gas, SiH$_4$, is very unstable and will decompose entirely. So the codeposition region becomes smaller going toward SiH$_3$Cl/NH$_3$ and so on, and is not present in the SiCl$_4$/NH$_3$ system. Another important feature to note is the occurrence of a large no-condensed-phase (ncp) region in the SiHCl$_3$/NH$_3$ and SiCl$_4$/NH$_3$ systems at higher temperatures, and the shrinking of the liquid silicon region.

As for the deposition efficiencies, the more chlorine the silane compound contains, the lower the deposition efficiencies, because of the larger stability with more chlorine. It is clear that when the Si/(Si + N) ratio decreases (i.e., the NH$_3$ concentration increases), the deposition efficiency rises. From the figures it also appears that increasing the temperature, in the temperature range below 1600 K, does not greatly affect the deposition efficiency. Here the contours are almost vertical. At higher temperatures the contours are seen to be more horizontal, and increasing the temperature lowers the deposition efficiency, by the appearance of stable high-temperature silicon-containing species. The deposition efficiencies in Kingon[1] are, in general, higher than our results, especially at higher Si/(Si + N) ratios, when the deposition efficiency is rising with increasing Si/(Si + N) ratio. These results seem more logical.

In Fig. 3 the partial pressures for the SiH$_4$/NH$_3$ and SiH$_2$Cl$_2$/NH$_3$ systems are shown, at a constant Si/(Si + N) ratio of 0.5. The silane system shows the almost complete conversion of silane in H$_2$ and formation of Si$_3$N$_4$ and Si. At high temperatures there is the occurrence of Si, SiH, Si$_2$, SiN, Si$_2$N, SiH$_2$, and Si$_3$, respectively, in decreasing quantities. The dichlorosilane system contains, apart from the product gases H$_2$ and HCl, more stable species like the chlorosilanes of which the SiCl$_4$ is the most stable. With increasing temperature, species like SiCl$_2$ gain importance, and at the highest temperatures SiCl becomes as important as SiCl$_2$. SiCl$_3$ is seen to be of no interest. Of the other silicon-containing species, there is the same order in occurrence as in the silane system. Of the newly included species, only SiHCl plays a role, especially at modest temperatures around 1700 K. Changing the Si/(Si + N) ratio does not affect these trends.

In the calculations of Kingon,[1] and in quite a number of older publications, SiCl$_3$ is the most important high-temperature radical, while in these calculations SiCl$_2$ and SiCl are dominant. This can be explained by the value of the heat of formation of SiCl$_3$ in the JANAF tables,[3] which is probably too negative. Hunt[11] discusses this problem.

While in Fig. 2 the CVD phase diagram of SiHCl$_3$/NH$_3$ is shown, in the next sections only the phase diagrams of SiH$_4$, SiH$_2$Cl$_2$, and SiCl$_4$ are shown, because the SiHCl$_3$ system is easily interpolated.

Table II. Values of Standard Entropy $S°$ and Standard Heat C_p of Formation in J/(K·mol) Interpolated by the Method Described by Hunt[33]

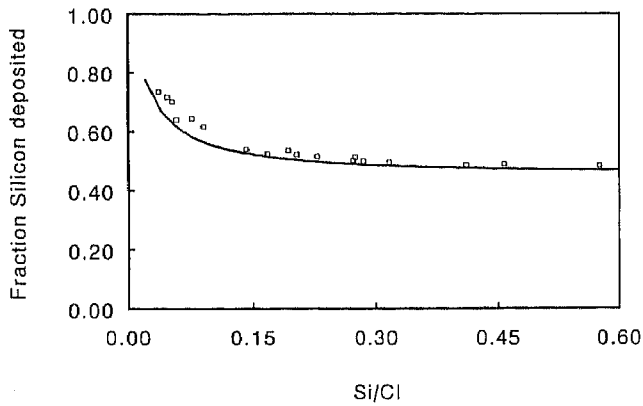| Species	$S°$	$C_p = A + BT + C/T^2$ (298–800 K)			C_p (800–2600 K)		
		A	$B \times 10^4$	$C \times 10^{-4}$	A	$B \times 10^5$	$C \times 10^{-5}$
SiH$_2$	200.29	28.47	240.9	−12.83	55.58	209.8	−65.61
SiH$_3$	202.50	31.73	391.8	−45.25	75.95	293.6	−107.8
SiHCl	249.01	32.65	129.2	−32.12	56.86	105.9	−37.84
SiHCl$_2$	290.40	63.72	153.3	−74.97	80.70	99.36	−45.13
SiH$_2$Cl	254.90	47.72	272.5	−60.11	78.33	196.5	−76.47

Fig. 1. Comparison of calculated and experimental[14] values of the deposition efficiency, as a function of the Si/Cl ratio in the input gas, at 1350 K: (□) Woodruff, experimental; (—) calculated.

(2) The Si–H–Cl–N System at Other Pressures

Raising the system pressure to 10 bar does not alter fundamentally the phase diagrams, as seen in Fig. 4. In general, below 1600 K there is little difference, both in the phase

boundaries and in the deposition efficiencies. At high temperatures the deposition efficiency is larger, and the maximum deposition efficiency has increased by 200 K. The figure of partial pressures gives exactly the same trends as in the 1-bar system.

Decreasing the system pressure to 1 mbar (Fig. 5) lowers the maximum deposition temperature by 400 K to about 1600 K. Because of this a solid Si area emerges. The Si_3N_4 area is now quite small. All silane homologues have large no-condensed-phase areas. As expected, the deposition efficiency decreases. The partial pressures show also some differences: the more prominent role of $SiCl_2$ at lower temperatures, but at higher temperatures $SiCl$ becomes more important and the $SiCl_2$ pressure decreases. Furthermore, at high temperatures the dominance of Cl, H, and gaseous Si has increased, while the other silicon-bearing species play a very minor role.

(3) The Si–H–Cl–N System in N_2 Dilution

From Fig. 6 it becomes clear that adding N_2 leads to the disappearance of the codeposition region, because now the nitrogen is available in sufficient quantities. There is also a small increase in the maximum deposition temperature and a decrease in the liquid Si region. At lower temperatures the
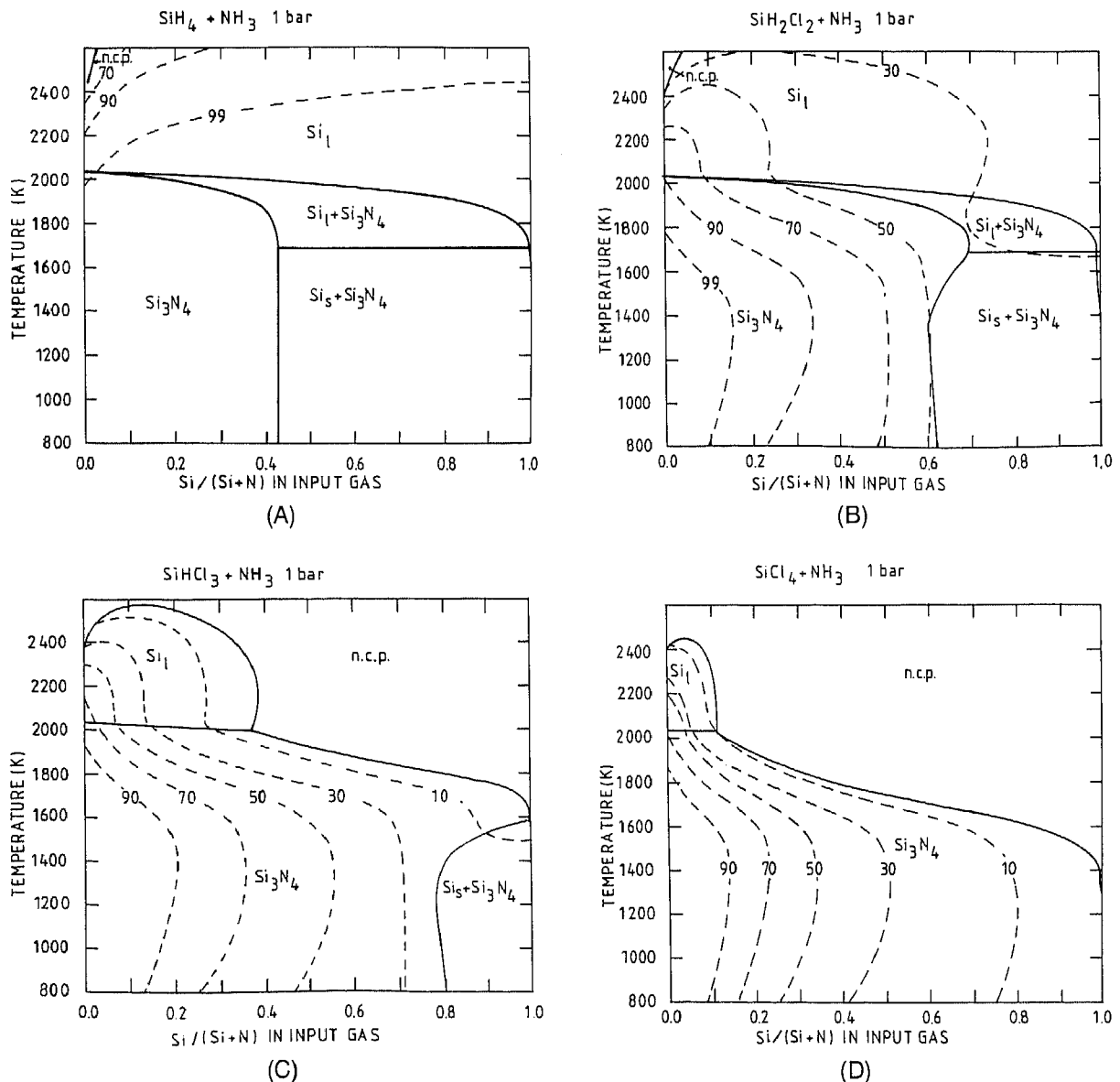
Fig. 2. CVD phase diagrams at 1 bar: (A) SiH_4/NH_3, (B) SiH_2Cl_2/NH_3, (C) $SiHCl_3/NH_3$, and (D) $SiCl_4/NH_3$.

SiH4+NH3 1 bar
Si/(Si+N)=0.5
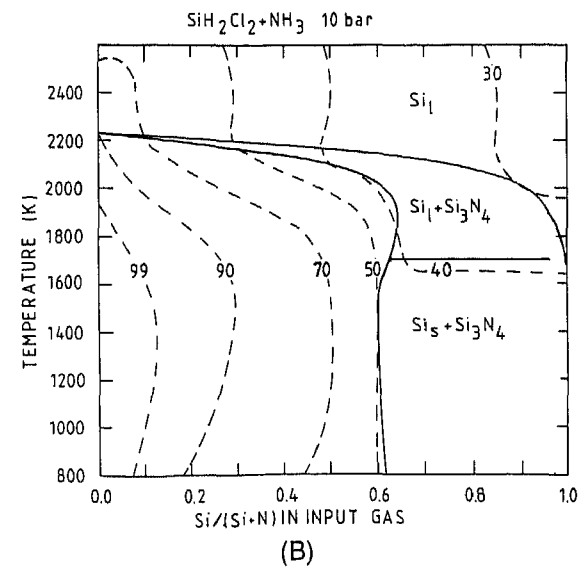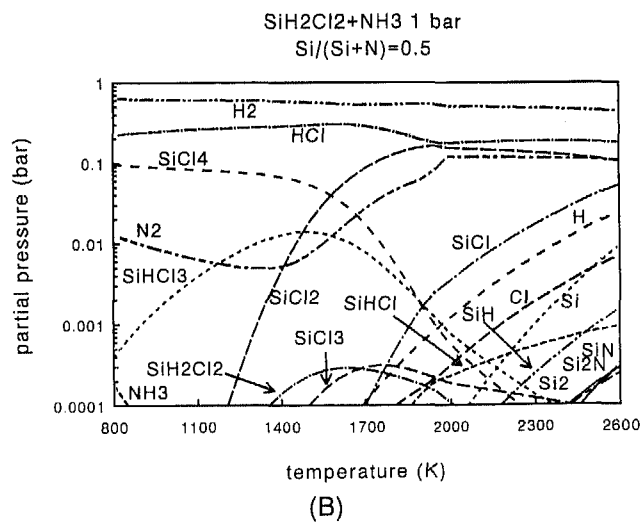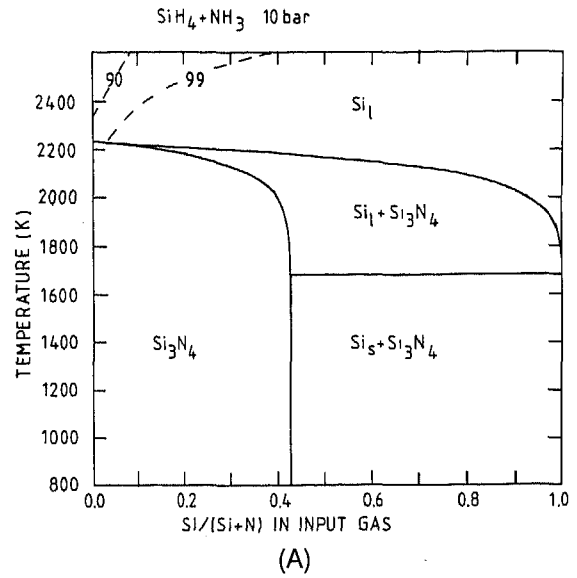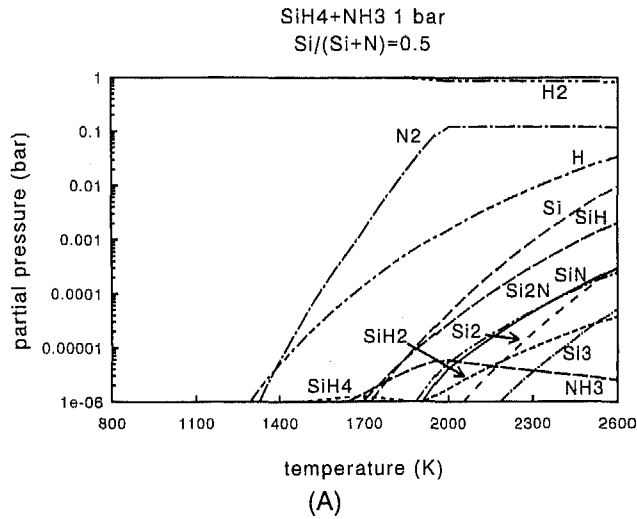

(A)

SiH2Cl2+NH3 1 bar
Si/(Si+N)=0.5

(B)

Fig. 3. Species partial pressures as a function of temperature, at Si/(Si + N) = 0.5. Pressure is 1 bar: (A) SiH_4/NH_3 and (B) SiH_2Cl_2/NH_3.

deposition efficiencies are higher but at very high temperatures, in the liquid Si area, these are lower and more horizontal, so changing the Si/(Si + NH_3) ratio does not have a great effect on the deposition efficiency. The temperature is more the controlling factor. The partial pressures are not fundamentally different, but at very high temperatures the concentrations of silicon-bearing species, like gaseous Si, SiH, SiN, Si_2N, and Si_2, are relatively larger than in the nitrogen-free system. This might account for the lower deposition efficiencies. It must be remembered that at lower temperatures kinetic retardation may occur,[1] and so the phase diagrams give the most favorable results because chemical equilibrium is assumed to be reached.

(4) The Si–H–Cl–N System in H_2 Dilution

Kinetic problems play a much less important role in the system diluted with H_2 (Fig. 7). A dilution factor of 10 lowers the maximum deposition temperature by about 100 K, but increases the deposition efficiency. At lower temperatures where Si_3N_4 is formed, the deposition efficiency is dependent mainly on the Si/(Si + N) ratio. At very high temperatures, when only liquid Si is present, it depends mainly on the temperature. The Si_3N_4 area has increased and in the $SiCl_4/NH_3$ system a large liquid Si area has developed. With a dilution factor of 1000 (Fig. 8) the phase diagrams of the different silanes look very much the same. The phase boundaries are identical above 1200 K and the deposition efficiencies of
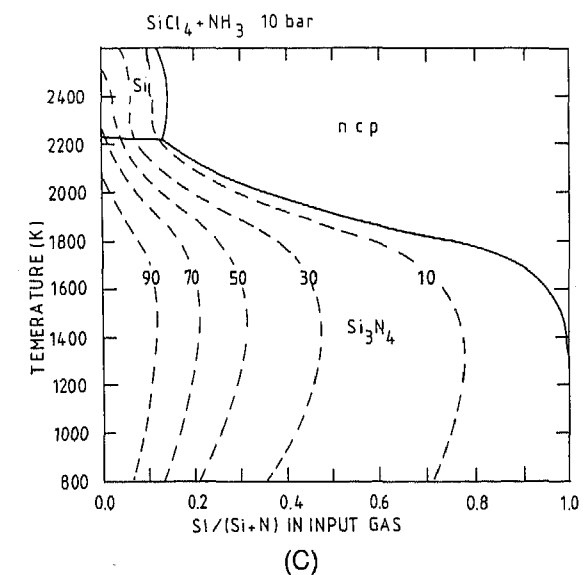
SiH_4+NH_3 10 bar

(A)

$SiH_2Cl_2+NH_3$ 10 bar

(B)

$SiCl_4+NH_3$ 10 bar

(C)

Fig. 4. CVD phase diagrams at 10 bar: (A) SiH_4/NH_3, (B) SiH_2Cl_2/NH_3, and (C) $SiCl_4/NH_3$.

Journal of the American Ceramic Society — Kruis et al.

SiH$_4$+NH$_3$ 1m bar

(SiH$_4$+NH$_3$)/N$_2$=10   1 bar

(A)

(A)

SiH$_2$Cl$_2$+NH$_3$ 1mbar

(SiH$_2$Cl$_2$+NH$_3$)/N$_2$=10   1 bar

(B)

(B)

SiCl$_4$+NH$_3$ 1m bar
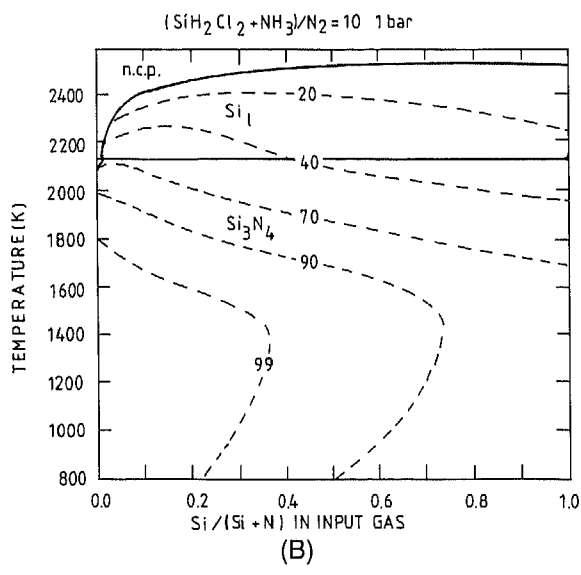
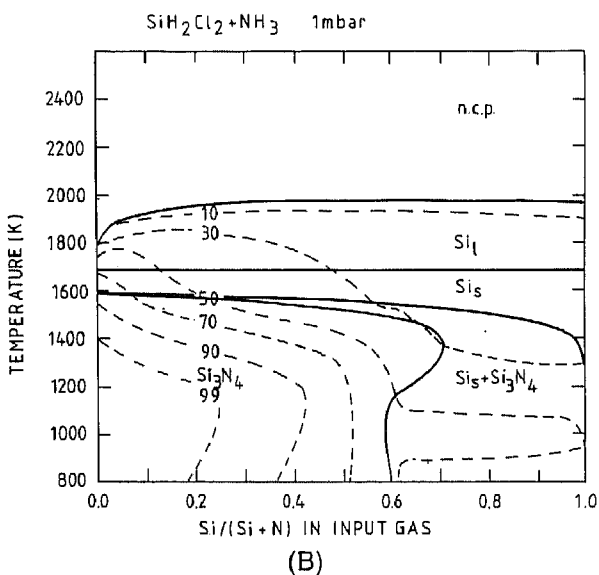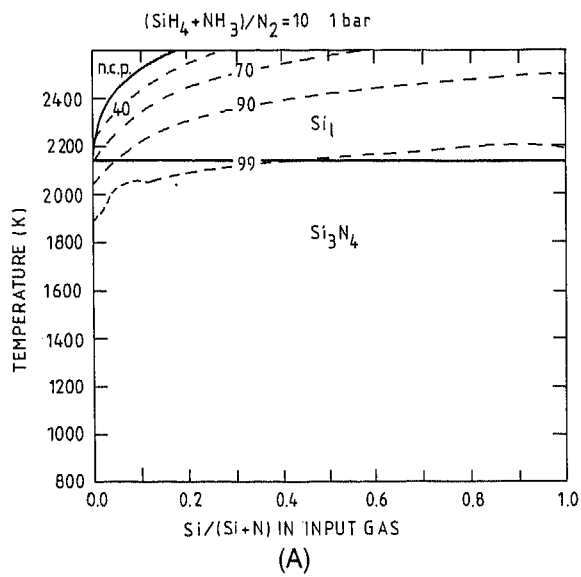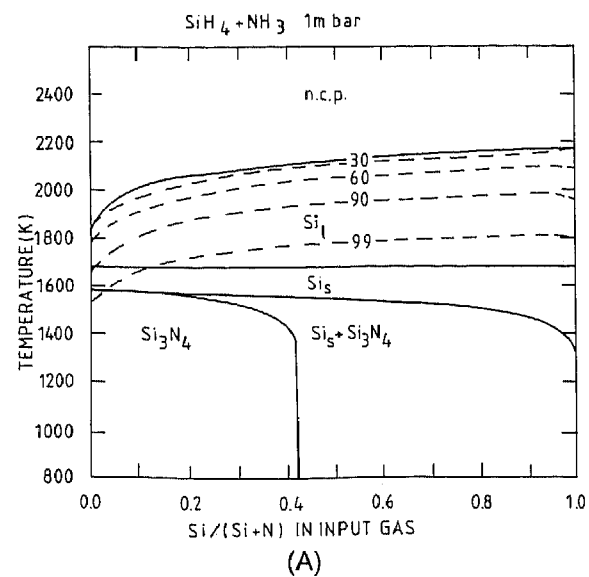(SiCl$_4$+NH$_3$)/N$_2$=10   1 bar

(C)

(C)
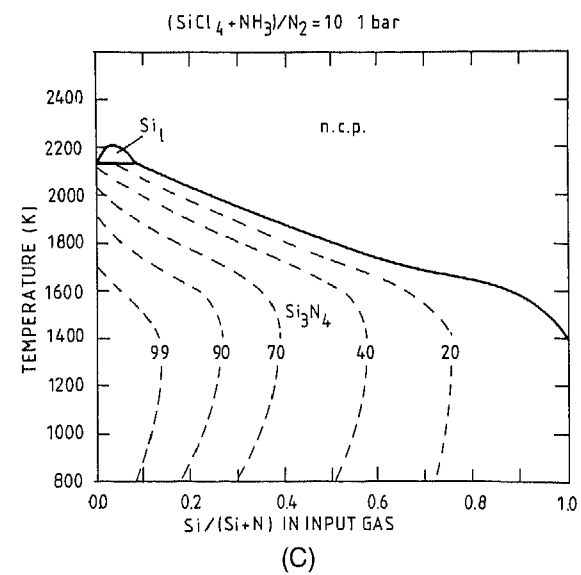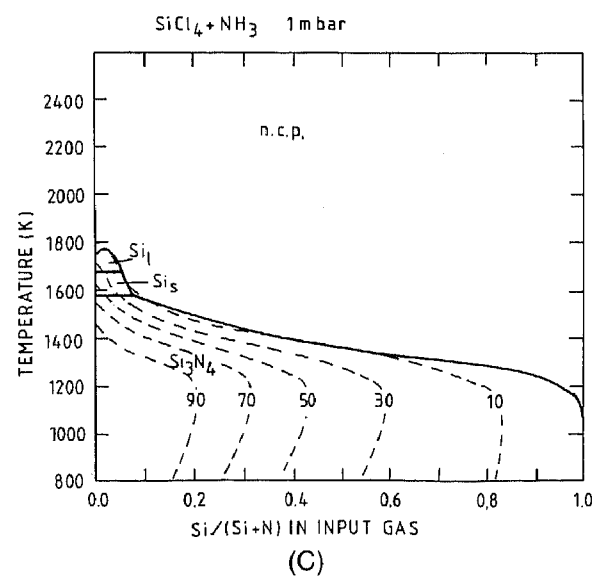
Fig. 5.   CVD phase diagrams at 1 mbar.

Fig. 6.   CVD phase diagrams with N$_2$ dilution: N$_2$/(Si + NH$_3$) = 10. Pressure is 1 bar.
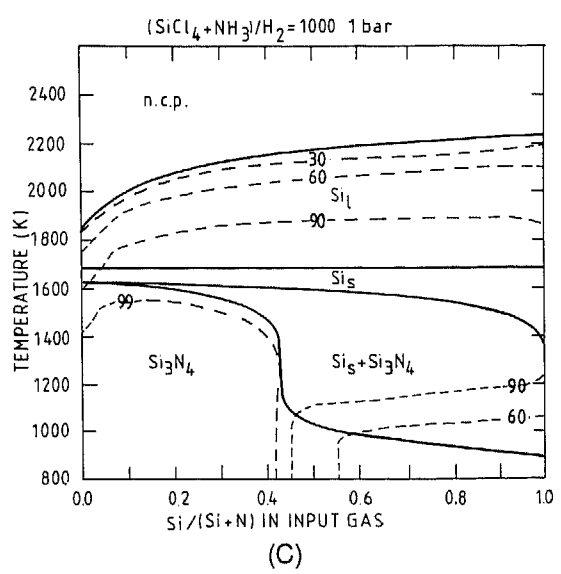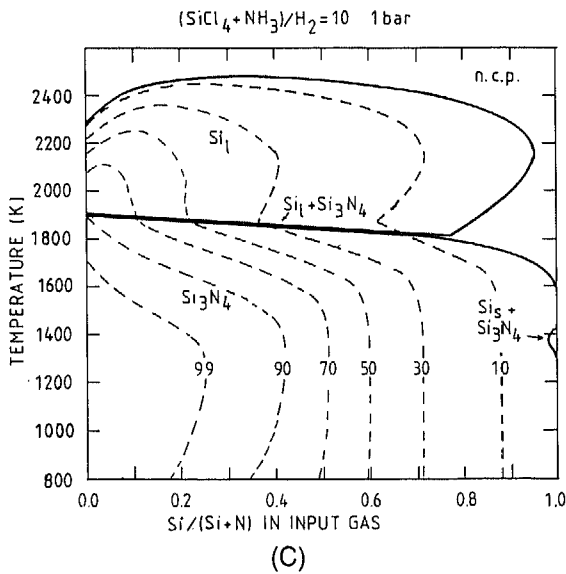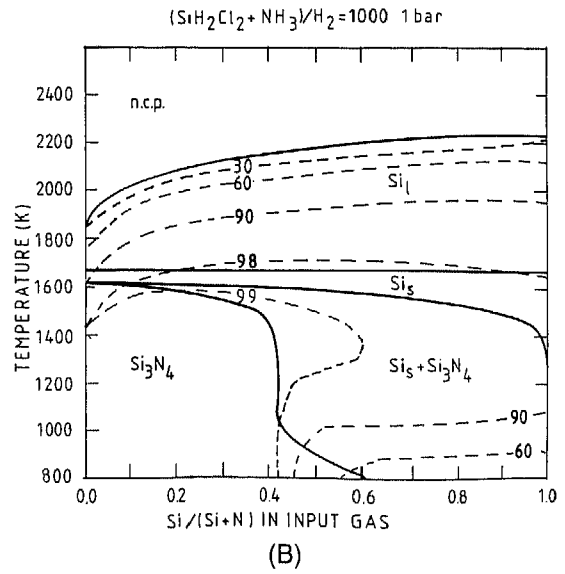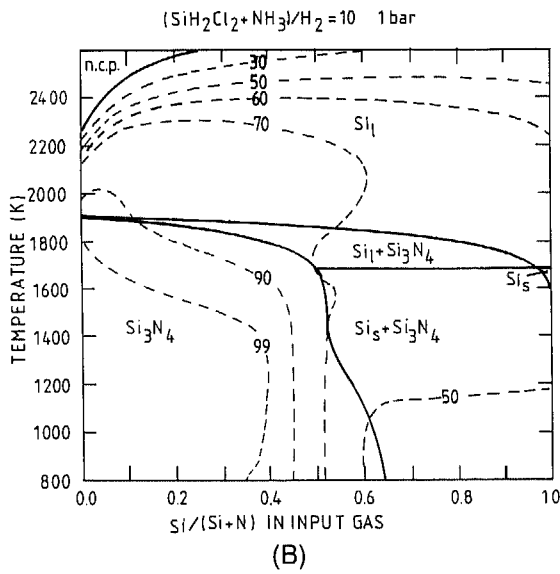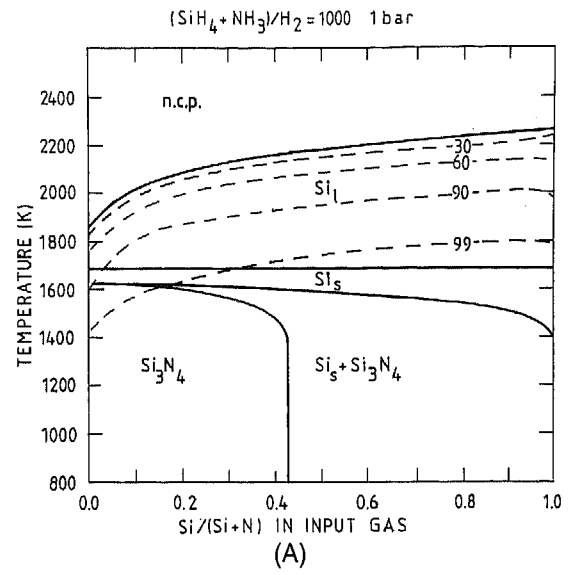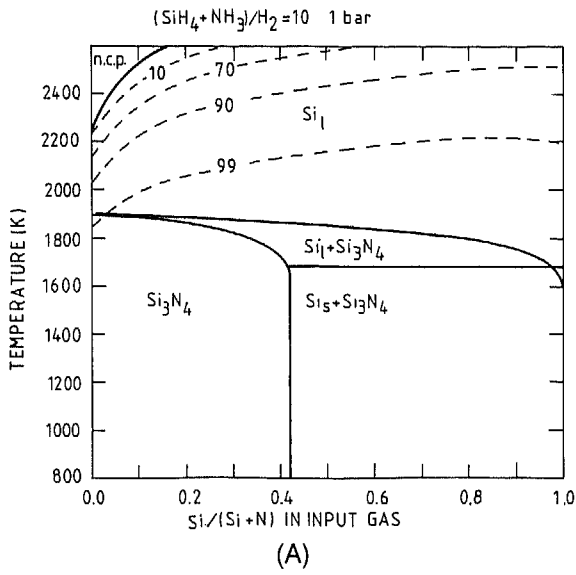
Fig. 7. CVD phase diagrams with H_2 dilution: $H_2/(Si + NH_3)$ = 10. Pressure is 1 bar.

Fig. 8. CVD phase diagrams with H_2 dilution: $H_2/(Si + NH_3)$ = 1000. Pressure is 1 bar.

SiH$_2$Cl$_2$/NH$_3$ and SiCl$_4$/NH$_3$ systems are almost identical. Now there is an appreciable codeposition region also in the SiCl$_4$/NH$_3$ system. The value of Si/(Si + N) = 0.43 (the Si–N stoichiometry of Si$_3$N$_4$) as a boundary is recognized. Looking at the partial pressures (Fig. 9), the surplus of H$_2$ results in low SiCl$_2$ and SiCl concentrations with SiCl as the most abundant species at high temperatures. Almost all of the silicon is incorporated into SiH; gaseous Si is even less available than Si$_2$.

In the case of SiH$_4$/NH$_3$, H$_2$ dilution has the same effect as lowering the system pressure, but this is in decreasing rate true for the chlorinated silanes, as can be seen in the different phase diagrams for the SiCl$_4$/NH$_3$ system at 1 mbar and high H$_2$ dilution (Figs. 5 and 8).

(5) Incorporating Si(NH)$_2$ in the Thermochemical Data Set

Using the estimations for the thermochemical data of Si(NH)$_2$ described in Section III, several phase diagrams were made. To gain insight into the reliability of these diagrams, several versions were made using different values of the heat of formation. Crosbie[17] gives a reliability of ±104.5 kJ/mol in the estimation of the heat of formation, and using this variation the phase diagrams change considerably. Using a value of −355.6 kJ/mol, there is a Si(NH)$_2$ region below 900 K at Si/(Si + N) values below 0.43 (SiH$_4$/NH$_3$) or 0.8 (SiCl$_4$/NH$_3$) (Fig. 10). When a higher value is used for the heat of formation (−251.1 kJ/mol), this region disappears, and using a lower value (−460.1 kJ/mol) the Si(NH)$_2$ region expands to 1600 K, creating a large Si/Si(NH)$_2$ codeposition region (Fig. 11). It is clear that the thermochemical data for Si(NH)$_2$ are not sufficiently reliable, but there is an indication that there is a Si(NH)$_2$ region at lower temperatures and lower Si/(Si + N) ratios.

(6) Using CVD Phase Diagrams in Understanding Synthesis Paths

This thermodynamic research arises from the experiments with different silanes in the laser-heated CVP reactor.[35–38] From these experiments it was concluded that understanding the thermodynamics is a first step in understanding the process. It is clear that the way in which the phase diagram is traversed is essential. At lower temperatures polymeric solid products like imides present a problem. This problem was solved by using a two-stage reactor: first heating the silane gas, without NH$_3$ present, and then adding the NH$_3$. In Fig. 12 this becomes clear in the phase diagram. First a liquid Si region is encountered, and the very small Si nuclei grow by coalescence of liquid drops and then these small Si particles come in contact with NH$_3$ and react. This is a fundamentally
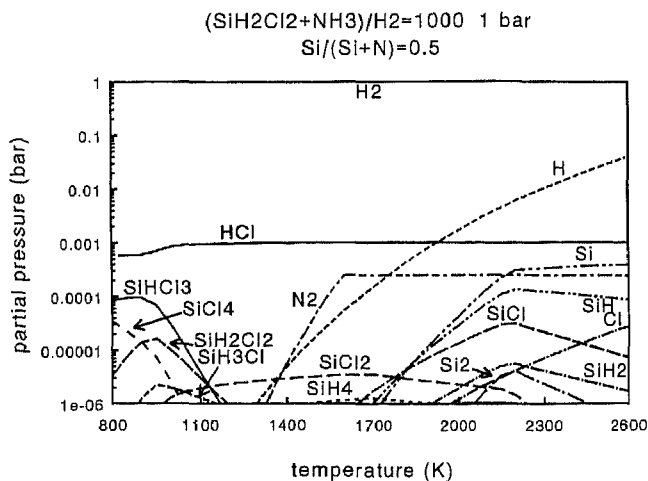
(SiH2Cl2+NH3)/H2=1000   1 bar
Si/(Si+N)=0.5

Fig. 9. Species partial pressures in the SiH$_2$Cl$_2$/NH$_3$ system as a function of temperature, at Si/(Si + N) = 0.5, and H$_2$/(Si + NH$_3$) = 1000. Pressure is 1 bar.

SiH$_4$+NH$_3$ 1 bar
including Si(NH)$_2$, ΔH_f^{298} = -355.6 kJ/mol

(A)

SiCl$_4$+NH$_3$ 1 bar
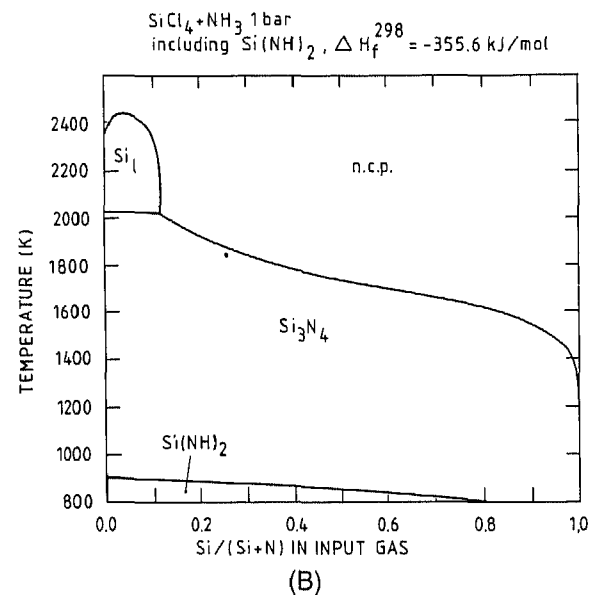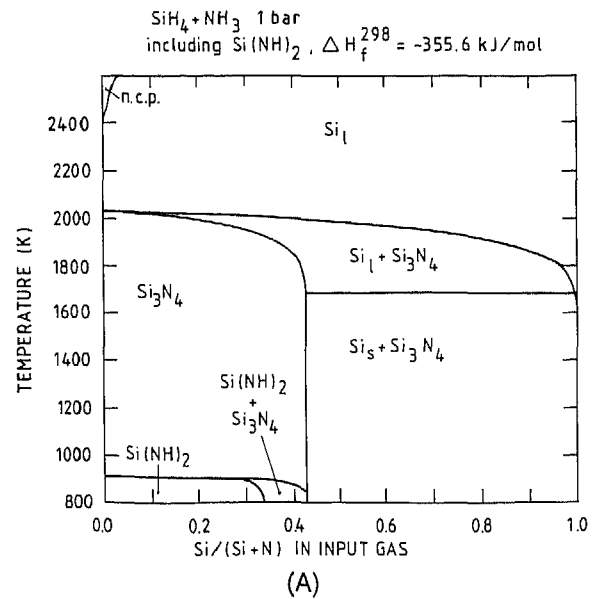including Si(NH)$_2$, ΔH_f^{298} = -355.6 kJ/mol

(B)

Fig. 10. CVD phase diagrams (without deposition efficiencies) including Si(NH)$_2$ (ΔH_{298} = −355.6 kJ/mol): (A) SiH$_4$/NH$_3$ and (B) SiCl$_4$/NH$_3$ at 1 bar.

different mechanism than by traversing first the probable solid imide region at low temperatures and then into the Si$_3$N$_4$ region. Looking at the CVD phase diagrams there are at least three possible ways of producing Si$_3$N$_4$: (1) with premixed reactants: coming through the probable solid silicon diimide (or similar polymeric intermediates) region, and from this formation of Si$_3$N$_4$ (path 1 in Fig. 12); (2) with a two-staged reactor: first heating up the (chloro)silane gas and then adding NH$_3$, or vice versa; (3) going through a no-condensed-phase region: formation of Si$_3$N$_4$ from the gas phase by homogeneous nucleation and growth (path 2 in Fig. 12); (4) going through a liquid Si region: reaction of NH$_3$ with liquid Si droplets, resulting in a porous particle (path 3 in Fig. 12). This is one of the reasons for extending the phase diagrams to high temperatures, where often no-condensed-phase regions are present. Passing through a no-condensed-phase region avoids undesirable imide formation and prevents formation of porous Si$_3$N$_4$ particles. Care must be taken to select a situation with a Si$_3$N$_4$ area with a high maximum deposition temperature, to get α- or β-Si$_3$N$_4$.
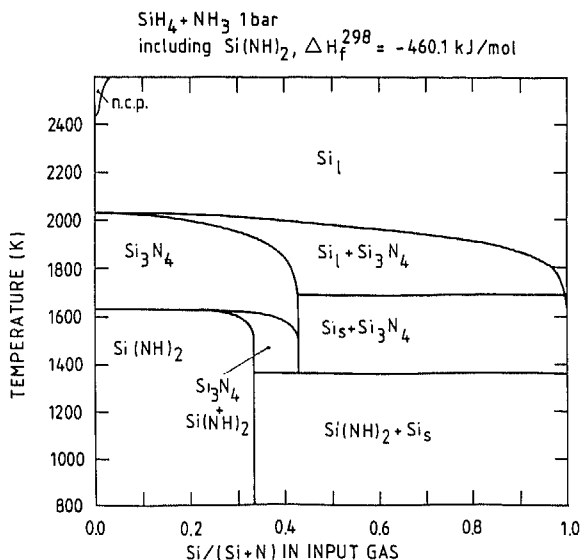
Fig. 11.   CVD phase diagram (without deposition efficiencies) including $Si(NH)_2$ ($\Delta H_{298} = -460.1$ kJ/mol) for SiH_4/NH_3 at 1 bar.

VI.   Conclusions

Thermodynamic equilibrium calculations are a useful tool in understanding the formation of Si_3N_4. With the CVD phase diagrams, and requirements on powder purity, porosity, particle size distribution, and process costs, a favorable synthesis path can be chosen. When a narrow particle size distribution and spherical, nonporous particles are desired, traversing through a low-temperature imide region or through a liquid silicon region should be avoided. The imide region can be avoided by allowing the (chlorinated) silane and the ammonia to mix only at higher temperatures. Avoiding the traverse of a liquid silicon region is more difficult. In the case of $SiCl_4$ and $SiHCl_3$, this can be achieved by adding ammonia at high temperature to the chlorinated silane. Conversely, in the case of SiH_4 and SiH_2Cl_2, the Si_3N_4 region is mostly bounded by a Si region. In that case, adding the (chlorinated) silane to the ammonia, and so coming from low Si/(Si + N) ratios at a temperature below the Si region, would be preferable. The figures in this article, with the full range of silane gases, extended toward high temperatures and, including the effects of pressure variation and H_2 or N_2 dilution, can be useful in selecting a particular synthesis path.
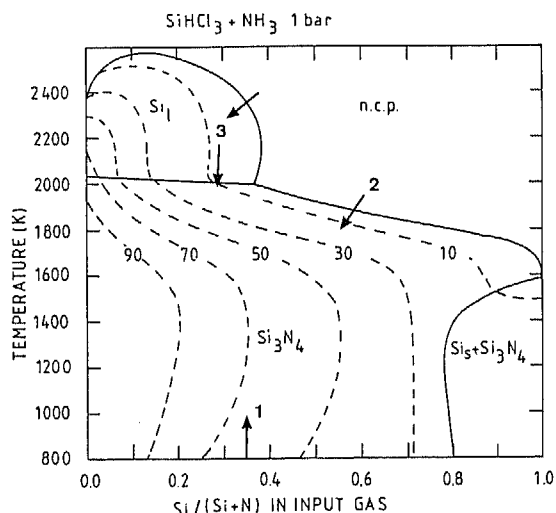

Fig. 12.   Possible routes of forming Si_3N_4: from an imide region, a silicon region, or from the gas phase.

For more chlorinated silanes, the deposition efficiency decreases, but the development of a no-condensed-phase area and shrinking of the Si/(Si + Si_3N_4) codeposition region might be favorable. Reducing the pressure lowers the maximum deposition temperature for Si_3N_4, which is not favorable for the formation of a crystalline phase. In the SiH_4 and SiH_2Cl_2 systems a no-condensed-phase region develops now also at higher temperatures, but is separated from the Si_3N_4 area by a Si region. Adding N_2 increases the deposition efficiency and leads to the disappearance of the codeposition region, but the effect is possibly less due to kinetic retardation. H_2 dilution leads to higher deposition efficiencies, but a larger codeposition area and a decrease in the maximum deposition temperature. At very high H_2 dilutions, the phase behavior of all the silane homologues is identical above 1200 K, where it is similar to that of SiH_4 at low pressure. As a general rule, at lower temperatures the Si/(Si + N) ratio is the most important factor for the deposition efficiency, while at higher temperatures the temperature becomes the controlling factor.

References

[1]A. I. Kingon, L. J. Lutz, and R. F. Davis, "Thermodynamic Calculations for the Chemical Vapor Deposition of Silicon Nitride," *J. Am. Ceram. Soc.,* 66 [8] 551–58 (1983).

[2]K. D. Allen and H. H. Sawin, "Thermodynamics of the Silicon-Chlorine–Hydrogen System: Chemical Potential for Homogeneous Nucleation," *J. Electrochem. Soc.,* 133 [2] 421–25 (1986).

[3]JANAF Thermochemical Tables, 3rd ed. Edited by Chase *et al.* National Bureau of Standards, Washington, DC, 1985.

[4]R. Walsh, "Thermochemistry of Silicon-containing Compounds," *J. Chem. Soc., Faraday Trans. 1,* 79, 2233–48 (1983).

[5]P. Ho, M. E. Coltrin, J. S. Binkley, and C. F. Melius, "A Theoretical Study of the Heats of Formation of SiH, SiCl, and SiHCl Compounds," *J. Phys. Chem.,* 89, 4647–54 (1985).

[6]P. Ho, M. E. Coltrin, J. S. Binkley, and C. F. Melius, "A Theoretical Study of the Heats of Formation of Si_2H (n = 0–6) Compounds and Trisilane," *J. Phys. Chem.,* 90, 3399–406 (1986).

[7]B. H. Boo and P. B. Armentrout, "Reaction of Silicon Ion (2P) with Silane (SiH_4, SiD_4). Heats of Formation of SiH, SiH (n = 1,2,3), and Si_2H (n = 0,1,2,3). Remarkable Isotope Exchange Reaction Involving Four Hydrogen Shifts," *J. Am. Chem. Soc.,* 109, 3549–59 (1987).

[8]M. E. Weber and P. B. Armentrout, "Energetics and Mechanisms in the Reaction of Si with $SiCl_4$. Thermochemistry of SiCl, SiCl, and $SiCl_2$," *J. Phys. Chem.,* 93, 1596–604 (1989).

[9]L. P. Hunt and E. Sirtl, "A Thorough Thermodynamic Evaluation of the Silicon–Hydrogen–Chlorine System," *J. Electrochem. Soc.,* 119 [12] 1741–45 (1972).

[10]E. Sirtl, L. P. Hunt, and D. H. Sawyer, "High Temperature Reactions in the Silicon–Hydrogen–Chlorine System," *J. Electrochem. Soc.,* 121 [7] 919–25 (1974).

[11]L. P. Hunt, "Thermodynamic Equilibria in the Si–H–Cl and Si–H–Br Systems," *J. Electrochem. Soc.,* 135 [1] 206–209 (1988).

[12]C. S. Herrick and R. A. Sanchez-Martinez, "Equilibrium Calculations for the Si–H–Cl System from 300 to 3000 K," *J. Electrochem. Soc.,* 121 [2] 455–58 (1984).

[13]V. S. Ban, "Chemical Processes in Vapor Deposition of Silicon," *J. Electrochem. Soc.,* 122 [10] 1389–91 (1975).

[14]D. W. Woodruff and R. A. Sanchez-Martines, "Experimental Study of Equilibrium Conditions in the Si–H–Cl System," *J. Electrochem. Soc.,* 132 [3] 706–708 (1985).

[15]T. Yoshida, H. Endo, K. Saito, and K. Akashi, "The Preparation of Ultrafine Si_3N_4 Particles in a Hybrid Plasma"; pp. 225–30 in the Proceedings of the 6th International Symposium on Plasma Chemistry, Montreal, Quebec, Canada, 1983; Vol. 1.

[16]R. Li and W. Gu, "Synthesis of Ultrafine and Ultrapure Silicon Nitride Powder in an RF-Plasma Furnace"; pp. 559–68 in *Production and Processing of Fine Particles.* Edited by A. J. Plumpton. Pergamon, New York, 1988.

[17]G. M. Crosbie, R. L. Predmesky, J. M. Nicholson, and E. D. Stiles, "Prepilot Scale Synthesis of Silicon Nitride under Pressure," *Am. Ceram. Soc. Bull.,* 68 [5] 100–14 (1989).

[18]S. Lin, "Mass Spectrometric Detection of Intermediates in Chemical Vapor Deposition of Si_3N_4 from $SiCl_4$ and NH_3," *J. Electrochem. Soc.,* 125 [11] 1877–79 (1978).

[19]A. Paretta, "Thermodynamic Calculations in the Chemical Vapour Deposition of Si_3N_4 from the NH_3–$SiCl_4$–H_2 System," *High Temp.— High Pressures,* 20, 97–107 (1988).

[20]J. B. Pedley and B. S. Iseard, CATCH Table for Silicon Compounds, University of Sussex, 1972, 1976. Available from National Technical Information Service, No. AD 773 468.

[21]T. N. Bell, K. A. Perkins, and P. G. Perkins, "Heats of Formation and Dissociation of Methylsilanes and Chlorosilanes and Derived Radicals," *J. Chem. Soc., Faraday Trans. 1,* 77, 1779–94 (1981).

[22]M. Farber and R. D. Srivastava, "Enthalpies of Formation of the Silane

Chlorides," *J. Chem. Thermodyn.* **11**, 939–44 (1979).

[23]M. Farber and R. D. Srivastava, "Mass Spectrometric Determination of the Heats of Formation of the Silicon Subchlorides $SiCl(g)$, $SiCl_2(g)$, and $SiCl_3(g)$," *J. Chem. Soc., Faraday Trans. 1*, **73**, 1672–80 (1977).

[24]W. C. Steele, L. D. Nichols, and F. G. A. Stone, "The Determination of Silicon–Carbon and Silicon–Hydrogen Bond Dissociation Energies by Electron Impact," *J. Am. Chem. Soc.*, **84**, 4441–45 (1962).

[25]J. L. Wang, J. L. Margrave, and J. L. Franklin, "Interpretation of Dissociative-Electron Attachment Processes for Silicon Tetrachloride," *J. Chem. Phys.*, **61**, 1357–60 (1974).

[26]P. Cadman, G. M. Tilsley, and A. F. Trotman Dickenson, "Abstraction of Chlorine Atoms from Alkyl Chlorides by the Trimethylsilyl Radical," *J. Chem. Soc., Faraday Trans. 1*, **69**, 914–21 (1973).

[27]R. Walsh, "Bond Dissociation Energy Values in Silicon-Containing Compounds and Some of Their Implications," *Acc. Chem. Res.*, **14** [8] 246–52 (1981).

[28]T. A. Carlson, N. Djuric, P. Erman, and M. Larsson, "New Predissociation in the A State in Silicon Hydride and Their Use in Deriving an Improved Value of the Dissociation Energy," *J. Phys. B*, **11**, 3667–75 (1978).

[29]J. A. Pople, B. T. Luke, M. J. Frisch, and J. S. Binkley, "Theoretical Thermochemistry. 1. Heats of Formation of Neutral AH Molecules (A = Li to Cl)," *J. Phys. Chem.*, **89**, 2198–203 (1985).

[30]S. K. Shin and J. L. Beauchamp, "Proton Affinity and Heat of Formation of Silylene," *J. Phys. Chem.*, **90**, 1507–509 (1986).

[31]J. Berkowitz, J. P. Greene, H. Cho, and B. Ruscic, "Photoionization Mass Spectrometric Studies of Silylidyne, Silylene, Silyl, and Silane (SiH (n = 1–4))," *J. Chem. Phys.*, **86** [3] 1235–48 (1987).

[32]K. S. Mazdiyasni and C. M. Cooke, "Synthesis, Characterization, and Consolidation of Si_3N_4 Obtained from Ammonolysis of $SiCl_4$," *J. Am. Ceram. Soc.*, **56** [1] 628–33 (1973).

[33]L. P. Hunt and E. Sirtl, "The Equilibrium Behavior of the Silicon–Hydrogen–Bromine and Silicon–Hydrogen–Iodine Systems," *J. Electrochem. Soc.*, **120** [6] 806–11 (1973).

[34]G. Eriksson, "Thermodynamic Studies of High Temperature Equilibria," *Chem. Scr.*, **8**, 100–103 (1975).

[35]R. A. Bauer, R. Smulders, J. G. M. Becht, P. J. van der Put, and J. Schoonman, "Laser-Chemical Vapor Precipitation of Submicrometer Silicon and Silicon Nitride Powders from Chlorinated Silanes," *J. Am. Ceram. Soc.*, **72** [7] 1301–304 (1989).

[36]R. A. Bauer, J. G. M. Becht, F. E. Kruis, B. Scarlett, and J. Schoonman, "Laser Synthesis of Low-Agglomerated Submicrometer Silicon Nitride Powders from Chlorinated Silanes," *J. Am. Ceram. Soc.*, **74** [11] 2759–68 (1991).

[37]F. E. Kruis, B. A. Scarlett, R. A. Bauer, and J. Schoonman, "Homogeneous Nucleation of Silicon in an Aerosol Reactor Using Laser-Heating"; pp. 210–13 in Aerosols, Science, Industry, Health and Environment, Proceedings of the Third International Aerosol Conference, Kyoto, Japan, September 24–27, 1990. Edited by S. Masuda and K. Takahashi. Pergamon Press, Oxford, U.K., 1990.

[38]F. E. Kruis, B. A. Scarlett, R. A. Bauer, and J. Schoonman, "Laser Synthesis of Sub-Micron Ceramic Powders"; pp. 321–28 in Proceedings of the Second World Congress, Particle Technology, Kyoto, Japan, Sept. 19–22, 1990. Society of Powder Technology, Kyoto, Japan, 1990.

[39]P. Gross, C. Hayman, and S. Mwroka, "Heat of Formation of Silicon Tetrachloride," *Trans. Faraday Soc.*, **65**, 2856–59 (1969).

[40]H. Schaefer and H. Heine, "Heats of Formation of $SiCl_4$, $SiBr_4$ and SiI_4," *Z. Anorg. Allg. Chem.*, **332**, 25–34 (1964).

[41]A. Schnegg, R. Rulaender, and H. Jacob, private communication (1986) to L. P. Hunt, in *J. Electrochem. Soc.*, **135** [1] 206–209 (1988).

[42]H. Seiter and E. Sirtl, "Removal of Si in the System Si–Cl–H," *Z. Naturforsch. A*, **21** [10] 1696–702 (1966).

[43]S. R. Gunn and L. P. Green, "The Heats of Formation of Some Unstable Gaseous Hydrides," *J. Phys. Chem.*, **65**, 779–83 (1961).

[44]H. Schaefer and J. Nickl, "On the Equilibrium Si + $SiCl_4$ = $2SiCl_2$ and the Thermochemical Properties of Gaseous Silicium(II)-chlorids," *Z. Anorg. Allg. Chem.*, **274**, 250–64 (1953).

[45]R. Teichmann and E. Wolf, "Experimental Research on the Equilibrium $SiCl_4(g)$ + $Si(s)$ = $2SiCl_2(g)$ According to the Flowmethod," *Z. Anorg. Allg. Chem.*, **347**, 145–55 (1966).

[46]H. Schaefer, H. Bruderreck, and B. Morcher, "The Thermochemistry of the Silicium(II)-Halogenides," *Z. Anorg. Allg. Chem.*, **352**, 122–37 (1967).

[47]M. J. S. Dewar, J. Friedheim, G. Grady, E. F. Healy, and J. J. P. Stewart, "Revised MNDO Parameters for Silicon," *Organometallics*, **5**, 375–79 (1986).

[48]E. Wolf and R. Teichmann, "On the Thermodynamics of the System Si–Cl–H," *Z. Anorg. Allg. Chem.*, **460**, 65–80 (1980). □